Earth and Planetary Science Letters 578 (2022) 117319

Contents lists available at ScienceDirect

Earth and Planetary Science Letters

www.elsevier.com/locate/epsl

Pb isotope insight into the formation of the Earth's first stable continents

Michael I.H. Hartnady [a,*], Christopher L. Kirkland [a], R. Hugh Smithies [c,a], Simon P. Johnson [c], Tim E. Johnson [b]

[a] Timescales of Mineral Systems Group, Curtin University, Perth, Australia
[b] School of Earth and Planetary Science, Curtin University, Perth, Australia
[c] Geological Survey of Western Australia, 100 Plain Street, East Perth, Australia

ARTICLE INFO

Article history:
Received 22 July 2021
Received in revised form 12 November 2021
Accepted 23 November 2021
Available online 8 December 2021
Editor: F. Moynier

Keywords:
early Earth
Pb isotopes
crustal evolution
Pilbara Craton
Eoarchaean

ABSTRACT

The formation of stable buoyant continental crust during the Archaean Eon was fundamental in establishing the planet's geochemical reservoirs. However, the processes that created Earth's first continents and the timescales over which they formed are debated. Here, we report the Pb isotope compositions of K-feldspar grains from 52 Paleoarchaean to Neoarchaean granites from the Pilbara Craton in Western Australia, one of the world's oldest and best-preserved granite–greenstone terranes. The Pb isotope composition of the Pilbara K-feldspars is variable, implying the granites were derived from crustal precursors of different age and/or variable time-integrated $^{238}U/^{204}Pb$ and $^{232}Th/^{204}Pb$ compositions. Trends to sub-mantle $^{207}Pb/^{206}Pb$ ratios preclude the influence of 4.3 Ga crustal precursors. In order to estimate crustal residence times we derive equations to calculate source model ages in a linearized Pb isotope evolution system. The best agreement between the feldspar Pb two-stage source model ages and those derived from zircon initial Hf isotope compositions requires crustal precursors that separated from a chondritic mantle source between 3.2 and 3.8 Ga, and rapidly differentiated to continental crust with $^{238}U/^{204}Pb$ and $^{232}Th/^{238}U$ ratios of ~14 and 4.2–4.5, respectively. The preservation of Pb isotope variability in the Pilbara Paleoarchaean granites indicates their early continental source rocks were preserved for up to 500 Ma after their formation. The apparent longevity of these early continental nuclei is consistent with the incipient development of buoyant melt-depleted cratonic lithosphere during the Eoarchaean to Paleoarchaean.

1. Introduction

Much of the preserved Archaean continental crust on Earth is comprised of rocks of the tonalite–trondhjemite–granodiorite (TTG) series, silica-rich sodic ($K_2O/Na_2O < 0.6$) granitic rocks with high Sr/Y and La/Yb ratios, and younger K-rich granitic derivatives (Moyen, 2011; Smithies et al., 2009). Although it is generally agreed that this early continental crust formed by partial melting of hydrated basaltic material at relatively high pressures (>0.7 GPa; Johnson et al., 2017) the age distribution of their source rocks and the geodynamic environment in which they formed is debated. Whereas some argue for an origin through partial melting of subducting hydrated oceanic lithosphere (Foley et al., 2002), others argue for intracrustal melting at the base of thickened volcanic plateaux (Smithies et al., 2009).

The Pilbara Craton in northwestern Australia is one of the world's oldest and best-preserved granite–greenstone terranes. The craton comprises Paleoarchaean to Mesoarchaean (~3.6–2.8 Ga) supracrustal sequences containing variably-differentiated volcanic and volcanoclastic rocks (the Pilbara Supergroup, Fig. 1), and near coeval plutonic complexes including rocks ranging in composition from primitive TTG to more K-rich monzogranite and syenogranite. The oldest components of these granite complexes appear to have formed through melting of thickened mafic crust in a non-subduction environment between 3.6 and 3.2 Ga (Van Kranendonk et al., 2007). Many of the Pilbara Paleoarchaean TTGs are generally too enriched in incompatible elements (K, U, Th, LILE, LREE) to have formed through melting of typical Archaean basaltic crust (Smithies et al., 2009). The 3.51 Ga mafic-to-intermediate volcanic rocks at the base of the Pilbara Supergroup (lower Warrawoona

* Corresponding author.
E-mail address: michael.hartnady@curtin.edu.au (M.I.H. Hartnady).

https://doi.org/10.1016/j.epsl.2021.117319

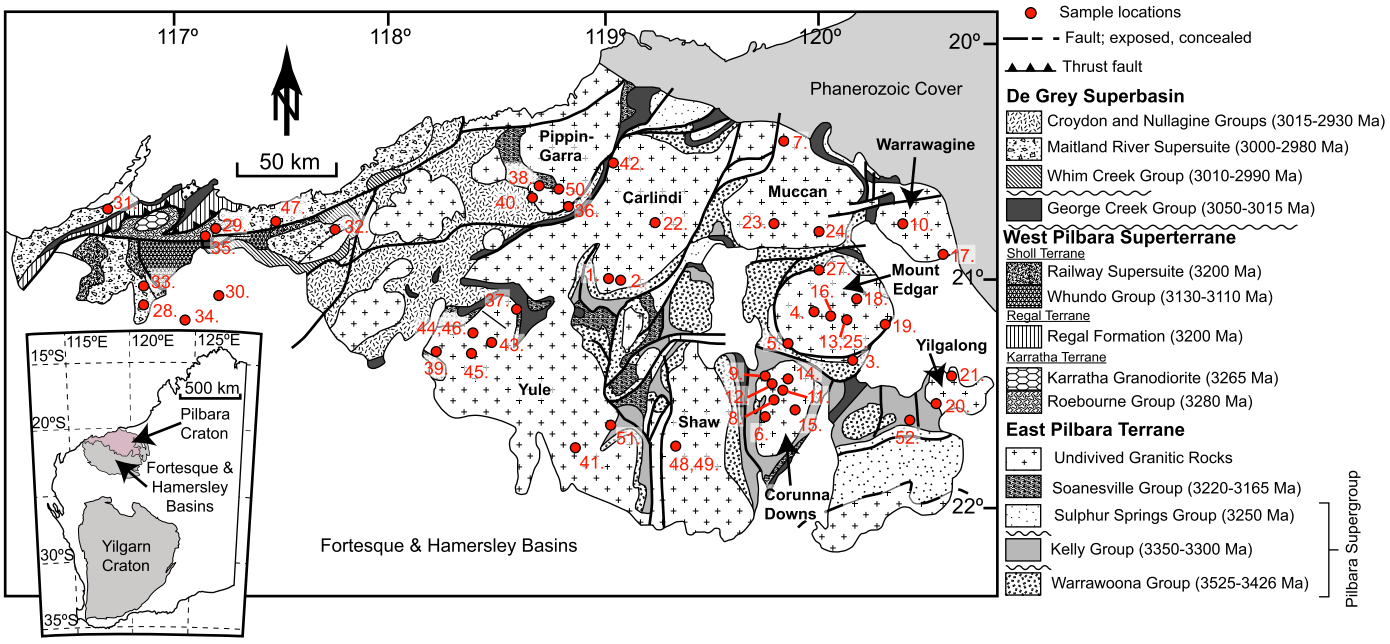

Fig. 1. Geological map of the Pilbara Craton (Kemp et al., 2015) showing the location of the 52 granite samples analysed for this study (red dots). Numbers associated with each sample locality refer to the map numbers (#) provided in Supplementary Dataset 1. (For interpretation of the colours in the figure(s), the reader is referred to the web version of this article.)

Group) are sufficiently enriched in incompatible elements to be the TTG source rocks (Smithies et al., 2009), and may represent a potential compositional analogue for Hadean-to-Eoarchaean protocrust. However, the age distribution of early crust in the Pilbara Craton, and hence rates of crustal growth and recycling during the early Archaean, are poorly constrained.

U–Pb and Hf isotope data from detrital zircon grains in Archaean sedimentary rocks and xenocrystic zircon crystals in various magmatic rocks from the Pilbara Craton show no evidence for the involvement of Hadean material (Kemp et al., 2015). Rather, such zircon data require extensive reworking of 3.8–3.6 Ga (Eoarchaean) crust, implying crustal residence times of 200 to 300 Myr assuming the crustal source was extracted from a depleted mantle reservoir (Gardiner et al., 2017). Other studies suggesting the earliest components of the Pilbara Craton were extracted from a chondritic mantle could imply even shorter residence times (Kemp et al., 2015; Petersson et al., 2019a, 2020). By contrast, the whole-rock Sm–Nd isotope compositions of 3.5 Ga sedimentary and volcanic rocks from the Warrawoona Group yield Nd isotopic compositions that indicate the source of these rocks separated from the mantle around 4.3 Ga (Tessalina et al., 2010). Although recent studies using ^{142}Nd suggest the Pilbara was not founded on a Hadean precursor (Archer et al., 2019; Murphy et al., 2021), these data could imply crustal residence times in excess of 800 Myr, and a protracted crustal prehistory that is absent from the zircon Hf isotopic record (Gardiner et al., 2017; Kemp et al., 2015).

The U–Th–Pb isotope system includes three discrete radioactive decay schemes (^{238}U–^{206}Pb, ^{235}U–^{207}Pb and ^{232}Th–^{208}Pb), and thus represents a powerful tool to unravel the processes and timescales of terrestrial differentiation, including crustal growth histories. Making even primitive granites, such as TTG, requires multi-stage partial melting of hydrated basaltic material (Johnson et al., 2017). The initial Pb isotopic composition of such granites will depend on the ^{238}U/^{204}Pb and ^{232}Th/^{204}Pb ratio of their source and the duration of radioactive decay prior to any remelting (Patterson and Tatsumoto, 1964). The mineral K-feldspar, which is a fundamental constituent of more evolved (i.e. potassic) felsic igneous rocks, is significantly enriched in Pb relative to U and Th such, that it records ^{238}U/^{204}Pb and ^{232}Th/^{204}Pb ratios close to zero (Gancarz and Wasserburg, 1977; Kramers and Tolstikhin, 1997). Consequently, post-crystallisation radiogenic ingrowth is generally negligible and the Pb isotopic composition of K-feldspar provides a close approximation for the initial Pb isotopic composition of the magma from which it grew. Thus, documenting natural variations in the ^{206}Pb/^{204}Pb, ^{207}Pb/^{204}Pb, and ^{208}Pb/^{204}Pb ratios in K-feldspar from upper crustal igneous rocks of varying age provides a potentially important means to discriminate their source components and evaluate crustal residence times (Kamber et al., 2003).

Here, we present new Pb isotopic data from K-feldspar grains from 52 samples of granite from the various magmatic complexes exposed across the Pilbara Craton. The magmatic crystallization ages of all samples have previously been determined through zircon U–Pb secondary ion mass spectrometry by the Geological Survey of Western Australia (https://catalogue.data.wa.gov.au/dataset/gswa-geochronology), and includes almost all of the major pulses of felsic magmatism in the region. The K-feldspar Pb isotope data is used to constrain the age and the ^{238}U/^{204}Pb (μ) and ^{232}Th/^{238}U (K) ratio of the magmatic sources, thereby providing insight into the source variability and differentiation history of some of Earth's oldest preserved continental crust.

2. Analytical methods

2.1. LA-ICP-MS analysis

Light mineral separates of granites and TTGs previously dated by zircon U–Th–Pb geochronology were mounted in 25 mm epoxy rounds and polished to approximately half grain thickness. A Tescan TIMA automated quantitative petrological analyser was used to characterise each sample. The characterisation procedure involved back-scattered electron (BSE) imaging at 1–3 µm resolution followed by energy dispersive X-ray spectroscopy (EDX) dot mapping with a 9 µm spacing. This characterisation process was used to identify K-feldspar grains suitable for isotopic analysis in order to avoid grains that were altered, contain cracks and/or inclusions, particularly those likely to host U and Th (e.g. zircon, monazite, apatite, etc, Supplementary Figures 1–5, Appendix A).

The Pb isotopic composition of K-feldspars were determined by laser-ablation inductively coupled plasma mass spectrometry (LA-ICP-MS) at the GeoHistory Facility in the John de Laeter Centre at Curtin University, Perth, Western Australia. Data were acquired over eight analytical sessions between January and May of 2020. Analyses were carried out on a Nu Plasma II (NPII) multi-collector mass spectrometer in conjunction with a Resonetics S-155-LR 193 nm excimer laser ablation system. K-feldspars were ablated using a 50 µm spot diameter, with a laser fluence between 2.2-2.5 J.cm^{-2}, as measured at the sample surface, and a pulse frequency of 10 Hz. Data acquisition consisted of two cleaning pulses, 20 s blank flush out, 40 s of baseline collection, 30 s ablation followed by 15 s of additional baseline collection. The sample cell was flushed with ultrahigh purity He (350 mL/min) and N_2 (1.0 mL/min) and high purity Ar was employed as the plasma carrier gas. Mass stations on the NPII were set as follows: ^{198}Hg, ^{200}Hg, ^{202}Hg, ^{203}Ti, ^{204}Pb + ^{204}Hg on ion counters; ^{205}Tl, ^{206}Pb, ^{207}Pb, and ^{208}Pb on Faraday cups with a 0.8 s integration time for all. Interference of ^{204}Hg on the 204 ion beam was corrected using a procedure similar to that described by Delavault et al. (2018), where the ^{204}Hg beam intensity was calculated based on the measured intensity of the interference free ^{202}Hg beam using the following equation:

$$I^{204}_{calculated} = I^{202}_{measured} \times \left[\frac{^{204}Hg}{^{202}Hg}\right]_{natural} \times \left(\frac{m_{^{202}Hg}}{m_{^{204}Hg}}\right)^{\beta}$$

Where β represents the exponential mass bias correction law (Russell et al., 1978) and the natural ratio ^{204}Hg/^{202}Hg is 0.22988 (Kent, 2008). The interference corrected intensity of the ^{204}Pb ion beam was calculated as follows:

$$I^{204}_{calculated} = \left[I^{^{204}Hg+^{204}Pb}\right]_{measured} - I^{204}_{calculated}$$

Normalisation was carried out using the matrix matched Shap K-feldspar (Tyrrell et al., 2006), analysed every 15-20 unknowns in a block with NIST 612 glass (n = 178 for all standards over the eight sessions). Data was reduced using Iolite 4 with an in-house data reduction scheme that yields Pb isotopic ratios and approximate Pb concentrations. The ^{206}Pb/^{204}Pb, ^{207}Pb/^{204}Pb and ^{208}Pb/^{204}Pb ratios of the unknown samples was calculated using standard sample bracketing.

$$\left(\frac{^{X}Pb}{^{204}Pb}\right)^{unknown}_{calculated} = \frac{\left(\left(\frac{I^{^{X}Pb}_{measured}}{I^{^{204}Pb}_{calculated}}\right)^{unknown} \times \left[\frac{^{X}Pb}{^{204}Pb}\right]^{Shap\ Kfs}_{reference}\right)}{mean\left(\frac{I^{^{X}Pb}_{measured}}{I^{^{204}Pb}_{calculated}}\right)^{Shap\ Kfs}}$$

Where ^{X}Pb denotes the ^{206}Pb, ^{207}Pb, or ^{208}Pb isotopes and the 'mean' refers to the value of a spline interpolated through the measured isotope ratio on the primary standard (Shap K-feldspar) at the relevant point in the time series, and is essentially equivalent to the average of the two bracketing standards.

During each analytical session, analyses of NIST612 when treated as an unknown yields isotopic ratios (^{206}Pb/^{204}Pb, ^{207}Pb/^{204}Pb and ^{208}Pb/^{204}Pb) within uncertainty of the published values (Tyrrell et al., 2006; Woodhead and Hergt, 2001). A summary of results for NIST612 during each session is provided in Supplementary Figure 6 and Supplementary Table 1. Although recent studies have reported minor inter-grain variability in Shap K-feldspar (Delavault et al., 2018), reduction of our data against NIST612 reveals all Shap analyses are consistent with published values and that any inter-grain heterogeneity is not resolvable at the level of precision for this study (Supplementary Fig. 7). Following data reduction, the data were filtered to remove analyses with high Hg, based on the ratio of calculated ^{204}Hg/^{204}Total > 0.2 in order to avoid analyses with large interference corrections that may show variations induced by differences in gains on the individual detectors (Paul et al., 2005). In addition, analyses with Pb concentrations less than 10 ppm were also discarded to exclude analyses with low signal to noise ratios and potentially mitigate effects of any radiogenic ingrowth in very low Pb grains. All corrected Pb isotope data for the standards and unknowns are provided in Supplementary Datasets 1 and 2 (Appendix B). Medians and standard errors for individual samples are reported in Supplementary Table 2 and Dataset 3.

3. Results

3.1. Pb isotope systematics in the Pilbara granites

Extracting information on the timescales of crust formation from the isotope systematics of crustal rocks requires a suitable mantle reference frame. In Supplementary Figure 8 Pb isotopic data are plotted in linear evolution diagrams of ^{x}Pb/^{204}Pb vs. exp($\lambda_x t$) with various mantle reference curves. We find that the single-stage Pb isotopic evolution model recently proposed by Maltese and Mezger (2020) with ^{238}U/^{204}Pb of 8.42 — as constrained by measurements on galena grains older than 3.2 Ga — provides a good approximation of the ^{206}Pb/^{204}Pb and ^{207}Pb/^{204}Pb compositions for the least radiogenic granites investigated in this study (Supplementary Fig. 8). Using the ^{232}Th/^{238}U value of 4.27 proposed by Maltese and Mezger (2020) yields ^{208}Pb/^{204}Pb compositions that are more radiogenic than many of the Pilbara granites (Supplementary Fig. 8). For the ^{232}Th–^{208}Pb system we therefore, revert to a ^{232}Th/^{238}U value of 4.03 (Maltese and Mezger, 2020), which provides a good approximation of the ^{208}Pb/^{204}Pb compositions for the least radiogenic Pilbara granites, and is also consistent with other estimates of Archaean mantle ^{232}Th/^{238}U ratios (Zartman and Richardson, 2005).

In the Pilbara Craton the Pb isotopic composition of the K-feldspar varies systematically with the crystallisation age of the granites and the long-term Pb isotopic evolution within Earth (Fig. 2a and b). The Pb isotope compositions of the granite-hosted K-feldspar also show identical distribution to that of galena ores from the Pilbara Craton (Supplementary Fig. 9). This observation indicates that the K-feldspar provides a good approximation of the initial Pb isotopic compositions of its host granite. That is, they have not been modified by significant in growth of radiogenic Pb since crystallization or had their Pb isotope system reset during latter thermal perturbations, and can be used to track crustal evolution. At an individual sample level this is reflected by the fact that the Pb isotopic signatures are close to those predicted by global Pb evolution models (e.g. Maltese and Mezger, 2020; Stacey and Kramers, 1975), and generally lie along two-stage paleogeochrons corresponding to the known zircon U–Pb crystallisation age of each sample (see Appendix C). Nevertheless, in all the Pb isotopic evolution diagrams there is significant scatter towards greater ^{206}Pb/^{204}Pb, ^{207}Pb/^{204}Pb, and ^{208}Pb/^{204}Pb values for granites of a given age (Fig. 2). There is also significant scatter in the ^{207}Pb/^{206}Pb compositions of both Paleoarchaean and Mesoarchaean granites (Fig. 2c).

Assuming a homogeneous mantle source, the ^{207}Pb/^{206}Pb ratio of a given granite is dependent on the ^{238}U/^{204}Pb ratio of the precursor crust from which the granite formed, and the time elapsed between initial separation of the basaltic source from mantle and its subsequent differentiation (remelting). Thus, granites formed by melting of a single homogeneous source will not produce significant ^{207}Pb/^{206}Pb variability. However, in the Pilbara Craton there is scatter towards lower ^{207}Pb/^{206}Pb ratios in almost all the magmatic events sampled (Fig. 2c), requiring some

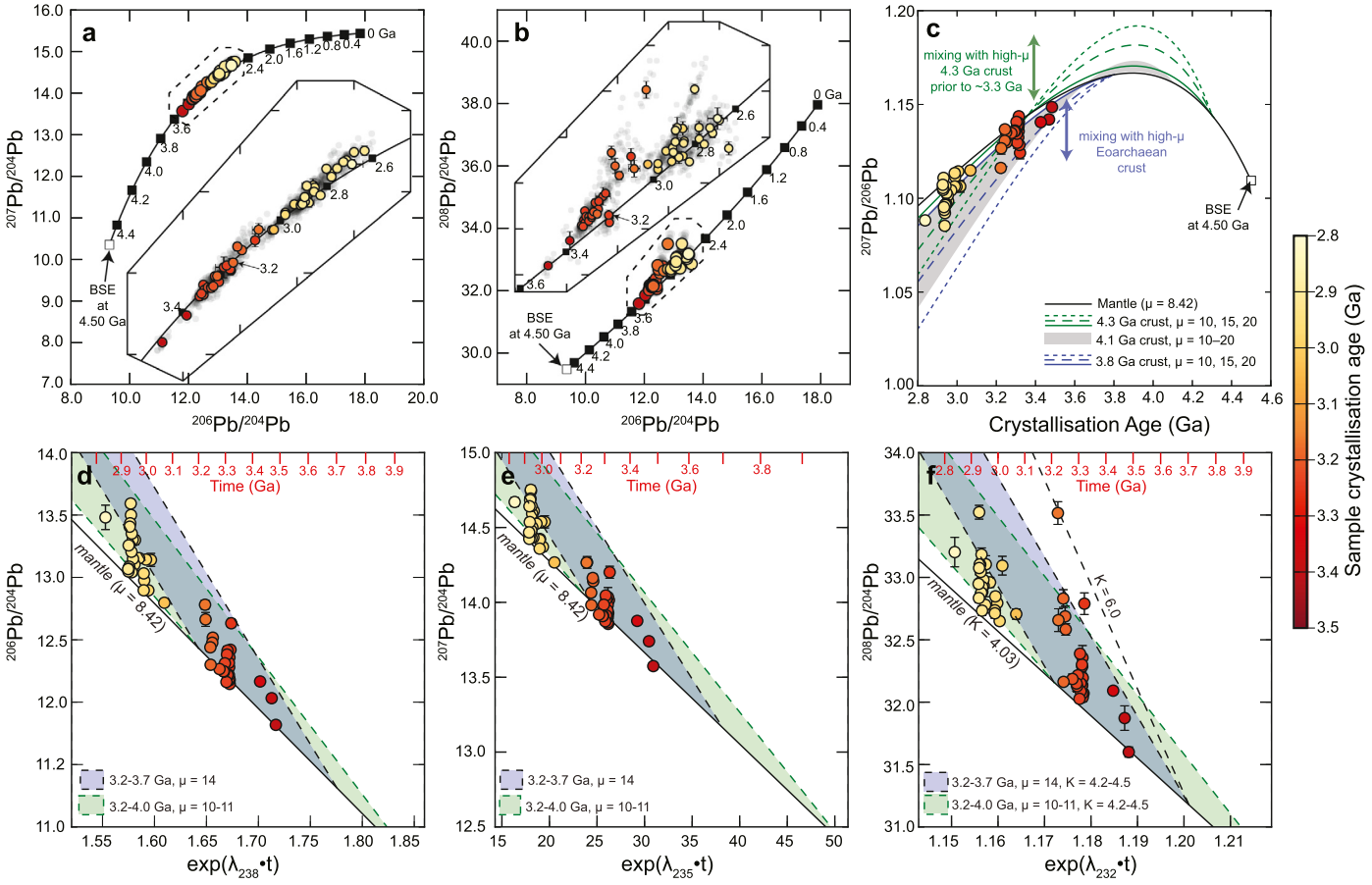

Fig. 2. a. $^{207}Pb/^{204}Pb$ vs. $^{206}Pb/^{204}Pb$. **b.** $^{208}Pb/^{204}Pb$ vs. $^{206}Pb/^{204}Pb$. **c.** $^{207}Pb/^{206}Pb$ vs. crystallization age. **d.** $^{206}Pb/^{204}Pb$ vs. $\exp(\lambda_{238}t)$. **e.** $^{207}Pb/^{204}Pb$ vs. $\exp(\lambda_{235}t)$. **f.** $^{208}Pb/^{204}Pb$ vs. $\exp(\lambda_{232}t)$ Grey dots denote individual K-feldspar analyses whereas coloured dots depict the average Pb isotope composition of each sample. The solid black curve illustrates the Archaean mantle Pb isotope evolution model ($^{238}U/^{204}Pb$ = 8.42, Maltese and Mezger, 2020). In panel c, green curves represent the Pb isotope evolution of hypothetical 4.3 Ga crustal reservoirs whereas blue curves denote hypothetical 3.8 Ga crustal reservoirs with $^{238}U/^{204}Pb$ from 10 to 20. Grey field denotes the Pb evolution of 4.1 Ga crust. Note that mixing with 4.3 Ga crust cannot produce the sub-mantle $^{207}Pb/^{206}Pb$ ratios observed in the Paleoarchaean Pilbara granites.

form of open system behaviour. Such Pb isotope heterogeneity has been observed in other Archaean crustal provinces and interpreted to indicate remelting and/or assimilation of differentiated high-$^{238}U/^{204}Pb$ material from a long-lived pre-existing protocrust, or inherited from a mantle with a heterogeneous Pb isotopic composition (Kamber et al., 2003; Kramers and Tolstikhin, 1997).

4. Discussion

4.1. Age of the high-U/Pb component

The Pb isotope variability of Paleoarchaean rocks from the North Atlantic Craton in West Greenland has been argued to reflect reworking of crust with a $^{238}U/^{204}Pb$ ratio of 10.5 that separated from the mantle in the Hadean, around 4.3 Ga (Kamber et al., 2003). Some whole-rock Sm-Nd data from the Warrawoona Group show evidence for an approximately 4.3 Ga source component for the Pilbara Craton (Tessalina et al., 2010). Evidence for a Hadean crustal component is also provided by detrital zircon grains in sedimentary rocks from the Mt. Narryer and Jack Hills supracrustal belts, and xenocrystic zircon in Paleoarchaean gneisses in the nearby Narryer Terrane, both of which form part of the Yilgarn Craton in Western Australia (Kemp et al., 2018; Petersson et al., 2019b). However, in the Pilbara Craton, both the oldest Hf model ages and the oldest zircon xenocrysts in magmatic rocks are around 3.8 Ga (Gardiner et al., 2017; Kemp et al., 2015). Therefore, on the basis of the zircon U–Pb and Hf isotope data, there is little evidence for significant volumes of Hadean material in the source of the Pilbara granites.

In the Hadean ^{235}U was more abundant than today. Since radioactive decay of ^{235}U (half-life ($T_{0.5}$) of ~0.7 Gyr) is about six times faster than ^{238}U ($T_{0.5}$) ~4.5 Gyr, the rate of production of ^{207}Pb exceeded that of ^{206}Pb. Consequently, the observed scatter towards lower $^{207}Pb/^{206}Pb$ (Fig. 2c) in the Pilbara granites is not consistent with derivation from Hadean material as old as 4.3 Ga. Such Hadean crust would have evolved to record a $^{207}Pb/^{206}Pb$ ratio significantly greater than coeval mantle (Fig. 2c), and would not have had sufficient time to produce enough ^{206}Pb to generate $^{207}Pb/^{206}Pb$ compositions as low as those observed for some of the Paleoarchaean granites from the Pilbara. It is possible that 4.1–4.0 Ga crust could produce the required $^{207}Pb/^{206}Pb$ compositions if this crust had $^{238}U/^{204}Pb$ of about 20 or more, whereas Eoarchean crust evolves to the lower $^{207}Pb/^{206}Pb$ compositions for $^{238}U/^{204}Pb$ ratios up to around 15 (Fig. 2c).

4.2. Origins of Pb isotopic variability

The extent to which the Pb isotopic variability reflects (i) the age and/or $^{238}U/^{204}Pb$ variability of source rocks in the Pilbara Craton, or; (ii) variable degrees of contamination of younger juvenile (mantle-like) melts by assimilation of older higher-$^{238}U/^{204}Pb$ felsic crust is difficult to constrain. Nevertheless, an attempt to distinguish between these two scenarios can be made based on the comparison of Pb isotope data with existing zircon Hf and O

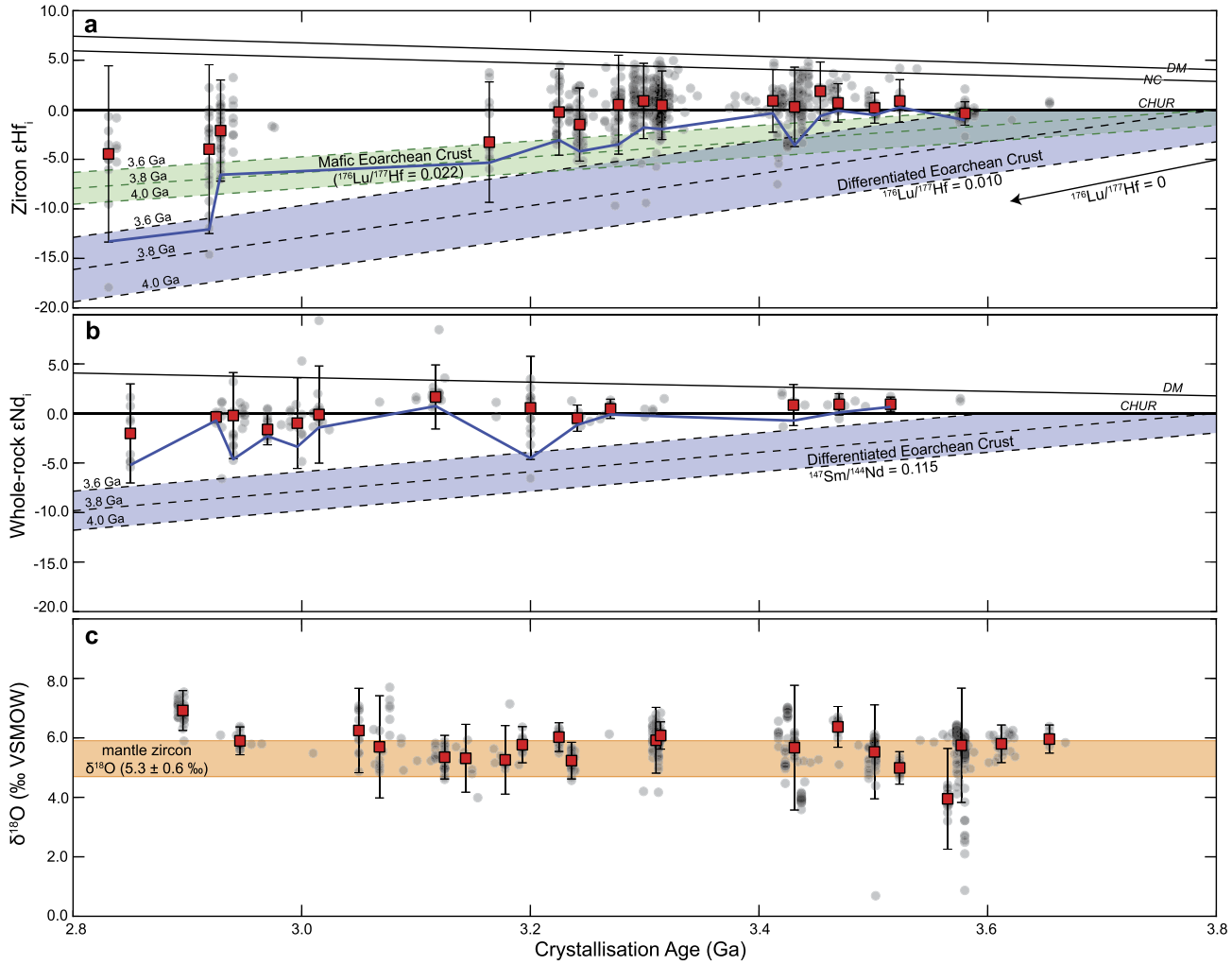

Fig. 3. Secular variation in zircon Hf-O, whole-rock Nd isotopic composition in the Pilbara Craton. Panels **a**, **b** and **c** show compilations of zircon initial Hf isotope compositions, whole-rock initial Nd isotope compositions and zircon oxygen isotopic compositions from the Pilbara Craton respectively. Red squares denote the 25 Myr running median compositions. Errors bars are 2SD. Chondritic uniform reservoir (CHUR) calculated using parameters of Bouvier et al. (2008) and decay constant of Söderlund et al. (2004). Depleted mantle reference curve (DM) calculated using parameters of Griffin et al. (2002). New crust reference curve (NC) calculated using parameters of Dhuime et al. (2011) Mantle zircon O isotope field after Cavosie et al. (2009). Solid blue lines in panels a and b represent the 5th percentile of initial zircon εHf and whole-rock εNd compositions in each 25 Myr bin respectively. Data were compiled from various published studies (Gardiner et al., 2017; Kemp et al., 2015; Petersson et al., 2019a, 2020; Smithies et al., 2009) along with regional datasets from the Geological Survey of Western Australia (https://dasc.dmp.wa.gov.au/dasc/).

isotopic data, whole-rock Nd isotopic data, and zircon inheritance patterns in the Pilbara Craton granites.

4.3. Mesoarchaean granites

If the Pb isotope variability of the Pilbara granites reflects variable degrees of contamination of juvenile magmas by older felsic crust, such variability should correlate with variations in zircon Hf and O isotopic compositions. Specifically, periods of greater crustal remelting/assimilation (lower εHf and higher δ^{18}O) should on average show both greater Pb isotope heterogeneity and more radiogenic Pb isotope compositions. By contrast, periods associated with greater degrees of mantle-derived magmatism should record less pronounced Pb isotope variability. A compilation of zircon Hf and O isotopic data from the Pilbara Craton (Fig. 3a and c) shows that the average zircon Hf isotopic composition of the Pilbara TTGs and granites are dominantly chondritic from 3.60 to 3.20 Ga (Fig. 3), indicating a dominance of new (juvenile) crustal growth during this period (Petersson et al., 2020, 2019a).

After 3.20 Ga, there is an increase in the proportion of zircon with subchondritic Hf isotopic compositions, indicating greater degrees of crustal remelting/assimilation (Gardiner et al., 2017). These data are consistent with oxygen isotope (δ^{18}O) compositions and inheritance patterns of zircon grains from the Pilbara Craton, which show a dominantly mantle origin from 3.6 to 3.1 Ga (Fig. 3b) and a secular shift to higher δ^{18}O composition at 3.1–3.0 Ga (Smithies et al., 2021), coupled with an increase in the abundance of Paleoarchaean and Mesoarchaean xenocrysts in granites over the same time interval (Supplementary Data 1). Therefore, the Pb isotopic variability in the Mesoarchaean granites (<3.2 Ga) must, to some extent, reflect remelting/assimilation of pre-existing Mesoarchaean to Paleoarchaean felsic crust.

4.4. Paleoarchaean granites

The older Paleoarchaean granites (>3.2 Ga) are characterised by a similar Pb isotope variability as their Mesoarchaean counterparts (Fig. 2). However, the Paleoarchaean granites have zircon Hf and O, and whole-rock Nd isotope compositions that are all mantle-like (Fig. 3), and these granites also generally contain fewer inherited zircon crystals (Supplementary Data 1).

In part, the differing degrees of isotopic heterogeneity exhibited by the Paleoarchaean granites reflect variable partitioning of the various parent and daughter elements during partial melting of the mantle, and their subsequent evolution within crustal and mantle reservoirs. For example, U, Th, and Pb are generally about two orders of magnitude more incompatible than Lu and Hf (or Sm and Nd) during partial melting of the mantle ($D_{U,Th,Pb} \sim 10^{-4}$ vs. $D_{Lu,Hf} \sim 10^{-1}$ to 10^{-2}) (White, 2020). Furthermore, the radioactive decay of ^{176}Lu ($T_{0.5} \sim 38$ Gyr) and ^{147}Sm ($T_{0.5} \sim 106$ Gyr) is at least an order of magnitude slower than that of ^{238}U ($T_{0.5} \sim 4.5$ Gyr) and almost two orders of magnitude slower than that of ^{235}U ($T_{0.5} \sim 0.7$ Gyr). Hence, the U-Pb isotope system is more sensitive to processes of fractionation and differentiation of the crust in the early Earth than other longer-lived isotope systems. This greater sensitivity reflects: (i) a greater enrichment factor of Pb than for Hf during extraction of crust from the mantle; and (ii) that differences in the Pb isotopic composition of the different reservoirs will diverge much more rapidly than their corresponding Hf (and Nd) isotopic compositions.

At face value, the zircon Hf isotope data could imply relatively continuous extraction of new crust from a primitive mantle reservoir (Petersson et al., 2020). However, the limited Hf isotope variability might indicate that insufficient time had elapsed for radiogenic ingrowth of Hf to generate measurable differences in the Hf isotope composition of the crust and mantle reservoirs, particularly if the early-formed protocrust was mafic with higher ^{176}Lu/^{177}Hf ratios than average felsic crust (Amelin et al., 1999). A regional compilation of whole-rock Nd isotope data also shows that Paleoarchaean magmatism tracks along a chondritic evolution (Fig. 3b). Although, in the case of the whole-rock Nd isotope data, the chondritic evolution might reflect a sampling bias towards more mafic rocks types. Consequently, the extent to which the early Pilbara crust was differentiated to more felsic compositions is unclear from the Hf and Nd isotope data alone.

In order to constrain the age distribution and ^{238}U/^{204}Pb (and ^{232}Th/^{238}U) composition of the Pilbara source rocks, we calculated two-stage Pb isotope source models ages for each of the analysed Palaeoarchaean granites (see Dataset 3). The term 'Pb model age' generally refers to an approximation of the crystallisation age of a sample based on its Pb isotope composition (Albarède et al., 2012; Milot et al., 2021). By contrast, our approach is analogous to two-stage depleted mantle model age calculations routinely performed in zircon Hf isotope studies (Belousova et al., 2010; Dhuime et al., 2012; Griffin et al., 2002). In the linearised Pb isotope evolution system of Albarede and Juteau (1984) the calculation of two-stage Pb source model ages can be conceptualised as the intersection point (I, J) of two straight lines, L_0 and L_1, describing the Pb isotope evolution of the reference reservoirs (e.g. bulk silicate Earth/depleted mantle) and crustal source reservoir respectively (see Supplementary Fig. 10). For this purpose, it is useful to describe the Pb isotope evolution of each reservoir using 'point-slope' form of the equation for a straight line:

$$L_0 : J - y_0 = m_0 (I - x_0) \quad \text{and}$$

$$L_1 : J - y_1 = m_1 (I - x_1) .$$

Here y_0 and y_1 denote the starting Pb isotope composition of the model and measured initial Pb isotope composition of the sample, m_0 and m_1 represent the parent–daughter ratio for the relevant Pb isotope system (e.g. ^{238}U/^{204}Pb, or μ, for the ^{238}U-^{206}Pb system) and x_0 and x_1 are related to the model starting time and crystallisations age of the sample respectively via the expression:

$$x = e^{(\lambda_x T)},$$

where λ_x denotes the relevant decay constant and T denotes time. As both lines share the common point (I, J) the two equations can be combined:

$$J = m_1 (I - x_1) + y_1 = m_0 (I - x_0) + y_0,$$

and solved for I;

$$I = \frac{(m_0 x_0 - m_1 x_1) + (y_0 - y_1)}{(m_0 - m_1)}$$

The x coordinate of the intersection point (I) represents the change point from the first stage evolution line to the second stage evolution line, and therefore provides an approximation of the time of extraction of the crustal source from the reference reservoir (T^2_{Res}):

$$T^2_{Res}\left(^{20x}Pb\right) = \frac{ln\,(I)}{\lambda_x}.$$

Assuming the source of the Pilbara granites had a ^{238}U/^{204}Pb composition of 10.5 (Kamber et al., 2003) yields Pb source models ages ranging from around 4.1 Ga to 3.2 Ga. Such a distribution of model ages is comparable to those obtained from initial zircon Hf isotope compositions assuming the crustal precursors were derived from a depleted mantle reservoir (black curve, Fig. 4a). However, zircon crystals with suprachondritic Hf isotope compositions (+ve εHf) are rare prior to 3.4 Ga (Fig. 3) and most recent studies indicate the earliest magmatism in the Pilbara Craton sourced a chondritic mantle from no earlier than around 3.8 Ga (Hawkesworth and Kemp, 2021; Petersson et al., 2019a, 2020).

However, if the source rocks for the Paleoarchaean granites had relatively high ^{238}U/^{204}Pb of 14 then their initial age variability is reduced, with calculated Pb source model ages ranging from 3.7 to 3.2 Ga (Fig. 4b). Kernel density estimates (KDE) of the K-feldspar Pb source model ages are nearly identical to those obtained from initial zircon Hf isotope data if the crustal sources were extracted from a mantle with chondritic Hf isotopic composition, with major peaks at 3.4 Ga and a subordinate peak between 3.7 and 3.6 Ga (Fig. 4b). This source model age distribution is also consistent with the lack of zircon xenocrysts older than about 3.7–3.6 Ga (Supplementary Dataset 1) (Kemp et al., 2015), and recent evidence for felsic magmatism extending back to ~3.6 Ga (Petersson et al., 2019a). Such variation in source age also accounts for most of the ^{208}Pb/^{204}Pb variability, with ^{232}Th/^{238}U values between 4.2 and 4.5, but rarely as high as 6.0 (Fig. 2f), which is consistent with the values observed in most upper crustal rocks globally (Wipperfurth et al., 2018). Hence, if one accepts that the oldest components in the Pilbara Craton were extracted from a chondritic mantle (Hawkesworth and Kemp, 2021; Petersson et al., 2020), then the Pb isotope data implies that the newly-formed mafic crust must have rapidly differentiated (within less than a few tens of millions of years) to more felsic compositions with higher ^{238}U/^{204}Pb ratios, before being isolated and subsequently reworked into the younger K-rich felsic magmas investigated in this work. Our data do not shed any light on the exact mechanism that drove this early crustal differentiation. However, one possible mechanism is fractional crystallisation of plagioclase, which preferentially incorporates Pb over U (Bédard, 2006), and would drive magmas to higher ^{238}U/^{204}Pb ratios. There is a systematic decrease in Eu/Eu* with increasing Rb/Sr for many of the younger plutonic rocks in the Pilbara Craton indicating plagioclase played an important role in their differentiation (Hawkesworth and Kemp, 2021).

An alternative interpretation is that the variability in the Pb isotope composition of the samples can be explained by re-melting of longer-lived mafic protoliths with inherent variation in the

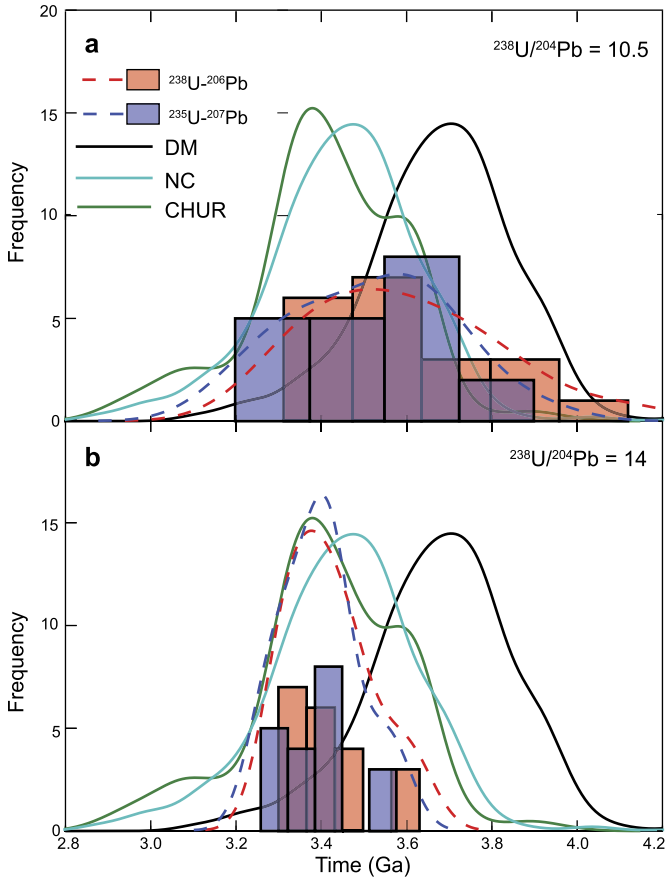

Fig. 4. Comparison of K-feldspar Pb and zircon Hf source model ages for Paleoarchaean granites in the Pilbara Craton. Histograms showing the distribution of two-stage source model ages derived from the Pb isotopic composition of K-feldspar from the Pilbara Craton. Red and blue colours correspond to ^{238}U–^{206}Pb and ^{235}U–^{207}Pb system respectively, for $^{238}U/^{204}Pb$ ratios of 10.5 and 14 (panels a and b). Green, cyan and black curves denote the distributions of zircon Hf two-stage source models ages when referenced to chondritic uniform reservoir (CHUR), new crust (NC), and depleted mantle (DM) respectively.

$^{238}U/^{204}Pb$ and $^{232}Th/^{204}Pb$ ratios (Fig. 2e). Inferring variably U- and Th-enriched source rocks for the Paleoarchaean granites is consistent with the observation that some of the oldest mafic rocks in the Pilbara Craton (lower Warrawoona Group) are enriched in K, LREE, and LILE relative to most Archaean basalts (Smithies et al., 2009). Previous authors have argued that the observed incompatible element enrichment of the lower Warrawoona Group basalts indicates derivation from a portion of the mantle that had been variably enriched through recycling of older felsic crust before 3.51 Ga (Smithies et al., 2009). However, such a model was not considered plausible for the Pb isotope variability in Archaean rocks from West Greenland, as a high-$^{238}U/^{204}Pb$ mantle reservoir would violate bulk Earth considerations (Kamber et al., 2003).

The geochemical and isotopic composition of modern-day ocean island basalts (OIB) and mid-ocean ridge basalts (MORB) demonstrates that the present-day mantle is heterogeneous (Doucet et al., 2020), and contains a radiogenic component (HIMU) that is believed to include recycled Archaean crust (Hofmann, 1997). The Sm–Nd and Rb–Sr isotope compositions of sub-calcic garnet inclusions in 3.3–3.2 Ga diamonds from Cretaceous kimberlites in Southern Africa indicate their growth in an enriched residual lithospheric mantle beneath the Kaapvaal Craton (Richardson et al., 1984). Furthermore, recent hydrogen and oxygen isotopic data from melt inclusions in olivine from 3.3–3.2 Ga komatiites from the Kaapvaal Craton indicates the presence of recycled near-surface materials and H_2O in the deep mantle source region of komatiites since at least the Paleoarchaean (Byerly et al., 2017; Sobolev et al., 2019). Therefore, it is plausible that incompatible element heterogeneity in the precursor mafic crust also contributed to some of the Pb isotopic variability in the granites.

5. Conclusions

The new K-feldspar Pb isotope data indicate that the crustal precursors for the Pilbara Craton could not have formed as early as 4.3 Ga and probably not before 3.8 Ga, consistent with recent studies showing $\mu^{142}Nd$ values similar to modern mantle and a paucity of Hadean zircon crystals (Gardiner et al., 2017; Kemp et al., 2015; Murphy et al., 2021). A novel application of source model age calculations to these Pb isotope data reveals strong agreement between K-feldspar Pb and zircon Hf source age distributions only if crustal sources were derived from a chondritic mantle and rapidly differentiated to more felsic compositions with $^{238}U/^{204}Pb$ around 14 and $^{232}Th/^{238}U$ between 4.2 and 4.5 during the Eoarchaean to Paleaoarchaean. These felsic crustal precursors must have been relatively long lived (up to 500 Myr) to develop the more radiogenic Pb isotope compositions and lower $^{207}Pb/^{206}Pb$ ratios preserved in younger Paleoarchaean granites of the craton.

For early continental crust to survive much of the Eoarchaean to Paleoarchaean transition and pass-on their radiogenic Pb signatures to younger magmas implies that early continental nuclei were able to resist recycling back into the mantle, and served as buoyant seeds for further crustal growth. An irreversible consequence of the extraction of Eoarchaean to Paleoarchaean crust from a primitive chondritic mantle is the formation a complementary buoyant melt-depleted mantle residue (Jordan, 1978), and recent work indicates the stabilisation of the early continents was coupled to the formation of this sub-continental lithosphere (Mulder et al., 2021 and references therein). Thus, the preservation of Pb isotopic variability in the Pilbara granites might reflect the incipient development of stable, melt-depleted, lithospheric mantle in the early Archaean.

Code availability

The Iolite code used for Pb isotope data reduction is available from the authors upon request or can be found at https://iolite.xyz/.

CRediT authorship contribution statement

Michael I.H. Hartnady: Conceptualization, Investigation, Methodology, Visualization, Writing – review & editing. **Christopher L. Kirkland:** Conceptualization, Resources, Validation, Writing – review & editing. **R. Hugh Smithies:** Conceptualization, Writing – review & editing. **Simon P. Johnson:** Conceptualization, Writing – review & editing. **Tim E. Johnson:** Validation, Writing – review & editing.

Declaration of competing interest

The authors declare that they have no known competing financial interests or personal relationships that could have appeared to influence the work reported in this paper.

Data availability

All new data generated in this study are provided in the Supplementary Information File and Supplementary Dataset. Regional compilations are available from the authors upon reasonable request.

Acknowledgements

This research was supported by an Australian Research Council (ARC) grant LP180100199 in conjunction with Northern Star Resources Ltd and the Geological Survey of Western Australia. TEJ acknowledges funding through Australian Research Council Discovery Project DP200101104 and support from the State Key Laboratory for Geological Processes and Mineral Resources, China University of Geosciences, Wuhan (Open Fund GPMR202101). The authors thank Brad J. McDonald and Noreen Evans for assistance in the JdLC analytical facilities. GeoHistory Facility instruments in the JdLC, Curtin University were funded via an Australian Geophysical Observing System grant provided to AuScope Pty Ltd. by the AQ44 Australian Education Investment Fund program. The JdLC GeoHistory laser ablation Facility is supported by AuScope and the Australian Government via the National Collaborative Research Infrastructure Strategy. Reviews by Sheree Armistead and an anonymous reviewer helped improve the paper. John Williams and the GSWA geochronology processing laboratory at Carlisle are sincerely thanked for facilitating this research by retrieving countless archived samples. Hugh Smithies and Simon Johnson publish with the permission of the Executive Director, Geological Survey of Western Australia.

Appendix. Supplementary material

Supplementary material related to this article can be found online at https://doi.org/10.1016/j.epsl.2021.117319.

References

Albarede, F., Juteau, M., 1984. Unscrambling the lead model ages. Geochim. Cosmochim. Acta 48, 207–212.
Albarède, F., Desaulty, A.M., Blichert-Toft, J., 2012. A geological perspective on the use of Pb isotopes in archaeometry. Archaeometry 54, 853–867.
Amelin, Y., Lee, D.-C., Halliday, A.N., Pidgeon, R.T., 1999. Nature of the Earth's earliest crust from hafnium isotopes in single detrital zircons. Nature 399, 252–255.
Archer, G.J., et al., 2019. Lack of late-accreted material as the origin of 182W excesses in the Archean mantle: evidence from the Pilbara Craton, Western Australia. Earth Planet. Sci. Lett. 528, 115841.
Bédard, J.H., 2006. Trace element partitioning in plagioclase feldspar. Geochim. Cosmochim. Acta 70, 3717–3742.
Belousova, E., et al., 2010. The growth of the continental crust: constraints from zircon Hf-isotope data. Lithos 119, 457–466.
Bouvier, A., Vervoort, J.D., Patchett, P.J., 2008. The Lu–Hf and Sm–Nd isotopic composition of CHUR: constraints from unequilibrated chondrites and implications for the bulk composition of terrestrial planets. Earth Planet. Sci. Lett. 273, 48–57.
Byerly, B.L., Kareem, K., Bao, H., Byerly, G.R., 2017. Early Earth mantle heterogeneity revealed by light oxygen isotopes of Archaean komatiites. Nat. Geosci. 10, 871–875.
Cavosie, A.J., Kita, N.T., Valley, J.W., 2009. Primitive oxygen-isotope ratio recorded in magmatic zircon from the Mid-Atlantic Ridge. Am. Mineral. 94, 926–934.
Delavault, H., Dhuime, B., Hawkesworth, C., Marschall, H.R., 2018. Laser-ablation MC-ICP-MS lead isotope microanalysis down to 10 µm: application to K-feldspar inclusions within zircon. J. Anal. At. Spectrom. 33, 195–204.
Dhuime, B., Hawkesworth, C.J., Cawood, P.A., 2011. When continents formed. Science 331, 154–155.
Dhuime, B., Hawkesworth, C.J., Cawood, P.A., Storey, C.D., 2012. A change in the geodynamics of continental growth 3 billion years ago. Science 335, 1334–1336.
Doucet, L.S., Li, Z.-X., El Dien, H.G., Pourteau, A., Murphy, J.B., Collins, W.J., Mattielli, N., Olierook, H.K., Spencer, C.J., Mitchell, R.N., 2020. Distinct formation history for deep-mantle domains reflected in geochemical differences. Nat. Geosci. 13, 511–515.
Foley, S., Tiepolo, M., Vannucci, R., 2002. Growth of early continental crust controlled by melting of amphibolite in subduction zones. Nature 417, 837–840.
Gancarz, A., Wasserburg, G., 1977. Initial Pb of the Amitsoq gneiss, West Greenland, and implications for the age of the Earth. Geochim. Cosmochim. Acta 41, 1283–1301.
Gardiner, N.J., et al., 2017. Processes of crust formation in the early Earth imaged through Hf isotopes from the East Pilbara Terrane. Precambrian Res. 297, 56–76.
Griffin, W.L., et al., 2002. Zircon chemistry and magma mixing, SE China: in-situ analysis of Hf isotopes, Tonglu and Pingtan igneous complexes. Lithos 61, 237–269.
Hawkesworth, C.J., Kemp, A.I.S., 2021. A Pilbara perspective on the generation of Archaean continental crust. Chem. Geol. 578, 120326.
Hofmann, A.W., 1997. Mantle geochemistry: the message from oceanic volcanism. Nature 219, 229.
Johnson, T.E., Brown, M., Gardiner, N.J., Kirkland, C.L., Smithies, R.H., 2017. Earth's first stable continents did not form by subduction. Nature 543, 239–242.
Jordan, T.H., 1978. Composition and development of the continental tectosphere. Nature 274, 544–548.
Kamber, B.S., Collerson, K.D., Moorbath, S., Whitehouse, M.J., 2003. Inheritance of early Archaean Pb-isotope variability from long-lived Hadean protocrust. Contrib. Mineral. Petrol. 145, 25–46.
Kemp, A.I.S., Wilde, S., Spaggiari, C.V., 2018. The Narryer Terrane, Yilgarn Craton, Western Australia: review and recent developments. In: Van Kranendonk, M.J., Bennett, V.C., Hoffmann, J.E. (Eds.), Earth's Oldest Rocks. Elsevier, Amsterdam, The Netherlands, pp. 401–433 (Chapter 18).
Kemp, A.I.S., Hickman, A.H., Kirkland, C.L., Vervoort, J.D., 2015. Hf isotopes in detrital and inherited zircons of the Pilbara Craton provide no evidence for Hadean continents. Precambrian Res. 261, 112–126.
Kent, A.J., 2008. In-situ analysis of Pb isotope ratios using laser ablation MC-ICP-MS: controls on precision and accuracy and comparison between Faraday cup and ion counting systems. J. Anal. At. Spectrom. 23, 968–975.
Kramers, J.D., Tolstikhin, I.N., 1997. Two terrestrial lead isotope paradoxes, forward transport modelling, core formation and the history of the continental crust. Chem. Geol. 139, 75–110.
Maltese, A., Mezger, K., 2020. The Pb isotope evolution of Bulk Silicate Earth: constraints from its accretion and early differentiation history. Geochim. Cosmochim. Acta 271, 179–193.
Milot, J., Blichert-Toft, J., Sanz, M.A., Fetter, N., Télouk, P., Albarède, F., 2021. The significance of galena Pb model ages and the formation of large Pb-Zn sedimentary deposits. Chem. Geol. 583, 120444.
Moyen, J.-F., 2011. The composite Archaean grey gneisses: petrological significance, and evidence for a non-unique tectonic setting for Archaean crustal growth. Lithos 123, 21–36.
Mulder, J.A., Nebel, O., Gardiner, N.J., Cawood, P.A., Wainwright, A.N., Ivanic, T.J., 2021. Crustal rejuvenation stabilised Earth's first cratons. Nat. Commun. 12, 1–7.
Murphy, D., et al., 2021. Combined Sm-Nd, Lu-Hf, and 142Nd study of Paleoarchean basalts from the East Pilbara Terrane, Western Australia. Chem. Geol. 578, 120301.
Patterson, C., Tatsumoto, M., 1964. The significance of lead isotopes in detrital feldspar with respect to chemical differentiation within the Earth's mantle. Geochim. Cosmochim. Acta 28, 1–22.
Paul, B., Woodhead, J.D., Hergt, J., 2005. Improved in situ isotope analysis of low-Pb materials using LA-MC-ICP-MS with parallel ion counter and Faraday detection. J. Anal. At. Spectrom. 20, 1350–1357.
Petersson, A., Kemp, A.I.S., Gray, C.M., Whitehouse, M.J., 2020. Formation of early Archean Granite-Greenstone Terranes from a globally chondritic mantle: insights from igneous rocks of the Pilbara Craton, Western Australia. Chem. Geol. 551, 119757.
Petersson, A., et al., 2019a. A new 3.59 Ga magmatic suite and a chondritic source to the East Pilbara Craton. Chem. Geol. 511, 51–70.
Petersson, A., Kemp, A.I.S., Whitehouse, M.J., 2019b. A Yilgarn seed to the Pilbara Craton (Australia)? Evidence from inherited zircons. Geology 47, 1098–1102.
Richardson, S.H., Gurney, J., Erlank, A., Harris, J., 1984. Origin of diamonds in old enriched mantle. Nature 310, 198–202.
Russell, W., Papanastassiou, D., Tombrello, T., 1978. Ca isotope fractionation on the Earth and other solar system materials. Geochim. Cosmochim. Acta 42, 1075–1090.
Smithies, R.H., Champion, D., Van Kranendonk, M.J., 2009. Formation of Paleoarchean continental crust through infracrustal melting of enriched basalt. Earth Planet. Sci. Lett. 281, 298–306.
Smithies, R.H., et al., 2021. Oxygen isotopes trace the origins of Earth's earliest continental crust. Nature 592, 70–75.
Sobolev, A.V., et al., 2019. Deep hydrous mantle reservoir provides evidence for crustal recycling before 3.3 billion years ago. Nature 571, 555–559.
Söderlund, U., Patchett, P.J., Vervoort, J.D., Isachsen, C.E., 2004. The 176Lu decay constant determined by Lu–Hf and U–Pb isotope systematics of Precambrian mafic intrusions. Earth Planet. Sci. Lett. 219, 311–324.
Stacey, J., Kramers, J., 1975. Approximation of terrestrial lead isotope evolution by a two-stage model. Earth Planet. Sci. Lett. 26, 207–221.
Tessalina, S.G., Bourdon, B., Van Kranendonk, M.J., Birck, J.-L., Philippot, P., 2010. Influence of Hadean crust evident in basalts and cherts from the Pilbara Craton. Nat. Geosci. 3, 214–217.
Tyrrell, S., Haughton, P., Daly, J., Kokfelt, T., Gagnevin, D., 2006. The use of the common Pb isotope composition of detrital K-feldspar grains as a provenance tool and its application to Upper Carboniferous paleodrainage, northern England. J. Sediment. Res. 76, 324–345.
Van Kranendonk, M.J., Smithies, R.H., Hickman, A.H., Champion, D., 2007. Secular tectonic evolution of Archean continental crust: interplay between horizontal

and vertical processes in the formation of the Pilbara Craton, Australia. Terra Nova 19, 1–38.
White, W.M., 2020. Geochemistry. John Wiley & Sons.
Wipperfurth, S.A., Guo, M., Šrámek, O., McDonough, W.F., 2018. Earth's chondritic Th/U: negligible fractionation during accretion, core formation, and crust–mantle differentiation. Earth Planet. Sci. Lett. 498, 196–202.
Woodhead, J.D., Hergt, J.M., 2001. Strontium, neodymium and lead isotope analyses of NIST glass certified reference materials: SRM 610, 612, 614. Geostand. Newsl. 25, 261–266.
Zartman, R.E., Richardson, S.H., 2005. Evidence from kimberlitic zircon for a decreasing mantle Th/U since the Archean. Chem. Geol. 220, 263–283.